

原位[2+3]环合成法制备四唑化合物、结构及荧光性质

谭育慧* 熊剑波 黄 珺 高继兴 徐 庆 于银梅 王 艳 杨 斌 舒 庆 唐云志*
(江西理工大学冶金与化学工程学院, 赣州 341000)

摘要: 利用氰基吡啶(4-氰基吡啶和 3-氰基吡啶)与稀土硝酸盐作用(Ln=Nd, Eu, Yb),通过原位[2+3]环加成反应合成得到了 4 个稀土四唑离子型化合物, $\text{Ln}(\text{H}_2\text{O})_8 \cdot 3(p\text{-TPD}) \cdot 2(p\text{-HTPD}) \cdot 7\text{H}_2\text{O}$, (Ln=Nd(**1**), Eu(**2**), Yb(**3**)), $p\text{-TPD}$ =4-tetrazolpyridine, $p\text{-HTPD}$ =protonated 4-tetrazolpyridine) 以及 $\text{Ln}(\text{H}_2\text{O})_8 \cdot 3(m\text{-TPD}) \cdot 6\text{H}_2\text{O}$ ($m\text{-TPD}$ =3-tetrazolpyridine, Ln=Yb(**4**)). X-射线单晶结构分析显示,在配合物 **1~4** 中,稀土金属离子与配体分别处于不同的两层, $[\text{Ln}(\text{H}_2\text{O})_8]^{3+}$ 结构单元与 $p\text{-TPD}$ 以及水分子通过氢键作用形成阳离子层(A 层),同时 $p\text{-TPD}$ 与 $p\text{-HTPD}$ 通过 $\pi\text{-}\pi$ 堆积与氢键作用形成阴离子层(B 层)。固态荧光分析表明,配合物 **1, 2, 4** 在 405、400、494 nm 处出现了最大强度的发射峰值;而配合物 **3** 在 618、592 及 462 nm 出现了最大强度的发射峰值。热重分析表明配合物 **1~4** 在 70~120 °C 范围内有 1 个失重,而在 180~220 °C 范围内配合物开始分解。

关键词: 四唑化合物; 镧系元素; 荧光性质; 晶体结构

中图分类号: O614.33 文献标识码: A 文章编号: 1001-4861(2014)07-1621-08

DOI: 10.11862/CJIC.2014.241

A Family of Tetrazole Compounds Formed Through *in situ* [2+3] Tetrazole Ligand Synthesis, Structures and Fluorescent Properties

TAN Yu-Hui* XIONG Jian-Bo HUANG Jun GAO Ji-Xing XU Qing YU Yin-Mei WANG Yan
YANG Bin SHU Qing TANG Yun-Zhi*

(School of Metallurgy and Chemical Engineering, Jiangxi University of Science and Technology, Ganzhou, Jiangxi 341000, China)

Abstract: Hydrothermal reaction of 4-cyanopyridine (or 3-cyanopyridine) and NaN_3 in the presence of Lewis acid lanthanide nitrate (Ln=Nd, Er, Yb) offers a serial of interesting ionic compounds $\text{Ln}(\text{H}_2\text{O})_8 \cdot 3(p\text{-TPD}) \cdot 2(p\text{-HTPD}) \cdot 7\text{H}_2\text{O}$, (Ln=Nd(**1**), Eu(**2**), Yb(**3**)), $p\text{-TPD}$ =4-tetrazolpyridine, $p\text{-HTPD}$ =protonated 4-tetrazolpyridine) and $\text{Ln}(\text{H}_2\text{O})_8 \cdot 3(m\text{-TPD}) \cdot 6\text{H}_2\text{O}$ ($m\text{-TPD}$ =3-tetrazolpyridine, Ln=Yb(**4**)). Single-crystal X-ray structure determination shows that all the compounds **1~3** exhibit ionic layer structure in which the vertical spread $p\text{-TPD}$ groups and the central metal cation $[\text{Ln}(\text{H}_2\text{O})_8]^{3+}$ constructed the cationic layer (A layer) through the hydrogen bonds among the $p\text{-TPD}$ groups and coordinated water molecules and the co-crystallized water molecules, part of the $p\text{-TPD}$ and $p\text{-HTPD}$ groups arrange along the zonal orientation formed the anionic layer (B layer) via $\pi\text{-}\pi$ stacking and hydrogen bonds. Compound **4** shows the similar ionic layer structure as compounds **1~3**. The solid-state fluorescence spectra of crystalline samples for **1~3**, and **4** indicate their maximal emission peaks occur in 405, 400 and 494 nm respectively, while compound **2** emits near-infrared luminescence with maximal emission peaks 618, 592 and 462 nm at room temperature. Thermo-gravimetric analysis (TGA) data shows all the compounds have a weightloss around 70~120 °C and start decomposition around 180~220 °C.

Key words: tetrazole compounds; lanthanide; fluorescent properties; crystal structure

收稿日期: 2013-08-19。收修改稿日期: 2014-02-11。

国家自然科学基金(No.21261009)江西省科技厅科技支撑计划研究项(20133BBE50020)国家 863 计划项目(2012AA061901)江西省教育厅科研项项目(GJJ13434)和江西理工大学博士启动基金(JXXJBS13003)资助项目。

*通讯联系人。E-mail: tyxen@163.com, Tel(Fax): +86-797-8312470

0 Introduction

Since pioneering work done by Sharpless et al.^[1], there have been tremendous research interests focused on the exploration of in situ tetrazole organic ligand synthesis through [2+3] cycloaddition reactions between organic cyano compounds and NaN_3 in the presence of Zn^{2+} ion as Lewis acid catalyst^[2-5]. Actually tetrazole organic ligand is prepared through the decomposition of Zn-complex (intermediate) under acidic conditions. As a result, there is much research focusing on the crystallographic characterization of such intermediates containing metal ion (most of them are metal-coordination polymers) and exploration of their applications in nonlinear optical, fluorescent (or phosphorescent), ferroelectric, and dielectric properties^[6-8]. Through the systematic investigations on the intermediates, it is well realized that the [2+3] cycloaddition reaction can occur between organic cyano groups and inorganic sodium azide (NaN_3) in the presence of transition metal ions as Lewis acid. So far, many transition metal ions such as Zn^{2+} ^[2-5], Cd^{2+} ^[9], Mn^{2+} ^[5,10], Cu^{2+} ^[9, 11], Ag^{+} ^[12], Co^{2+} ^[10,13], Pd^{2+} ^[14] acting as Lewis acid have been reported; however, there is few report about single Ln^{3+} ^[15] as Lewis acid to mimic Sharpless tetrazole synthesis reaction. To the best of our knowledge, only Li Liang et al reported a series of novel three-dimensional (3D) Ln(III)-Cu(I) heterometallic tetrazole-based coordination frameworks by using Ln^{3+} as catalyst^[15].

As a continuation of systematic investigations about the trapping, crystallographic characterization, and applications of these intermediates by using Ln^{3+} as Lewis acid catalyst, we adopt another reaction condition by combination of hydrothermal reaction and programmed cooling methods. As shown in scheme 1, when we selected 4-cyanopyridine or 3-cyanopyridine as reaction substrate, used Ln^{3+} to replace the transition metal ions, adopted a programmed cooling method after the [2+3] cycloaddition reactions (hydrothermal reaction), we successfully obtained the crystalline samples of the reaction product. To our surprise, totally different from other tetrazole complexes^[1-15], all the

compounds (**1**, **2**, **3**, **4**) we got exhibit the interesting ionic layer structures, in which all the central metal cations $[\text{Ln}(\text{H}_2\text{O})_8]^{3+}$ can be viewed as “A” layers, and part of the p-HTPD and *p* (or *m*)-TPD anions can be viewed as “B” layers. The “A” and “B” layers are cross-linked each other by hydrogen bonds. Herein, we reported the synthesis, crystal structure, fluorescent properties and thermo-gravimetric curves of these title intermediates.

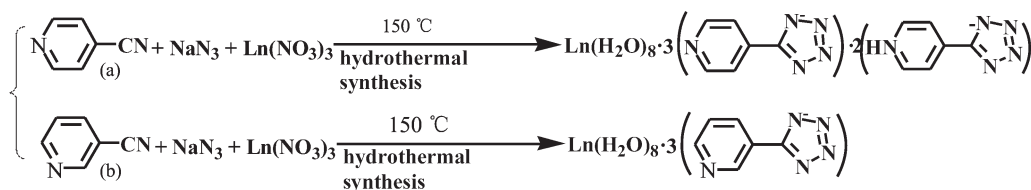
1 Experimental

1.1 Materials and methods

All reagents and solvents employed were commercially available and used without further purification. The C, H and N microanalyses were carried out with a Vario EL elemental analyzer. The IR spectra were recorded with a Nicolet Avatar 360 FTIR spectrometer using the KBr pellet technique. Thermogravimetric curves were measured on a Perkin-Elmer TGA-7 (USA) at a heating rate of $10\text{ }^\circ\text{C}\cdot\text{min}^{-1}$ from room temperature to $800\text{ }^\circ\text{C}$ under air.

1.2 Synthesis of compounds 1~4

As shown in scheme 1, compounds **1**~**3** were prepared under hydrothermal reaction condition. A heavy walled Pyrex tube containing a mixture of 4-cyanopyridine ($\text{Nd}(\text{NO}_3)_3\cdot 6\text{H}_2\text{O}$ (0.066 g, 0.2 mmol) or $\text{Eu}(\text{NO}_3)_3\cdot 6\text{H}_2\text{O}$ (0.068 g, 0.2 mmol) or $\text{Yb}(\text{NO}_3)_3\cdot 6\text{H}_2\text{O}$ (0.072 g, 0.2 mmol) and water (2.5 mL) was frozen and sealed under vacuum, then placed them inside an oven at $150\text{ }^\circ\text{C}$ for 3 d and then cooled to room temperature at a rate of $5\text{ }^\circ\text{C}\cdot\text{h}^{-1}$. The purple block crystals for **1**, pale yellow crystals for **2**, and colorless block crystals for **3** were obtained by filtration. The same procedures were conducted for **4** by using 3-cyanopyridine (0.0208 g, 0.2 mmol) replaced 4-cyanopyridine. The pale green crystals for **4** were afforded by filtration. For **1**, $\text{C}_{30}\text{H}_{52}\text{N}_{25}\text{O}_{15}\text{Nd}$ (1 147.21) Yield: 23.2%. Calcd. (%): C, 31.38, H, 4.53; N, 30.51; Found (%): C, 31.21; H, 4.47; N, 30.56. For **2**, $\text{C}_{30}\text{H}_{52}\text{N}_{25}\text{O}_{15}\text{Eu}$ (1 154.93) Yield: 27.2%. Calcd. (%): C, 31.17; H, 4.50; N, 30.30; Found (%): C, 31.15; H, 4.46; N, 31.12, For **3**, $\text{C}_{30}\text{H}_{52}\text{N}_{25}\text{O}_{15}\text{Yb}$ (1 176.01) Yield: 26.5%. Calcd. (%): C, 30.61; H, 4.42; N, 29.76; Found (%): C, 30.65; H, 4.42; N, 29.77. For

Scheme 1 (a) Preparation of compounds **1**~**3**, Ln=Nd (**1**), Eu(**2**), Yb(**3**); (b) Preparation of compounds **4**, Ln=Yb

4, C₁₈H₄₀ErN₁₅O₁₄ (863.69) Yield: 23.2%. Calcd. (%): C, 25.01; H, 4.63; N, 24.31; Found (%): C, 24.98; H, 4.66; N, 24.32.

1.3 Single crystal structure determination

Single crystal of compounds **1**~**4** were selected on a Bruker Smart Apex CCD diffractometer with graphite-monochromated Mo K α radiation ($\lambda=0.071\ 073\ \text{nm}$) at 293 K using the φ - ω scan technique. Absorption corrections were applied using SADABS^[16]. The structures were solved by direct methods using the

program SHELXS-97 and all the non-hydrogen atoms were refined anisotropically on F^2 by the full-matrix least-squares technique using the SHELXL-97 crystallographic software package^[17]. All the hydrogen atoms were positioned geometrically and refined using a riding mode. Detailed information about the crystal data and structure determination for title complexes are summarized in Table 1. Their selected intra atomic distances and bond angles are given in Table S I. Hydrogen bonds summarized in Table S II.

Table 1 Crystal data and structure refinement for **1**~**4**

Complex	1	2	3	4
Empirical formula	C ₃₀ H ₅₂ NdN ₂₅ O ₁₅	C ₃₀ H ₅₂ EuN ₂₅ O ₁₅	C ₃₀ H ₅₂ YbN ₂₅ O ₁₅	C ₁₈ H ₄₀ YbN ₁₅ O ₁₄
Formula weight	1 147.21	1 154.93	1 176.01	863.69
Crystal system	Triclinic	Triclinic	Triclinic	Triclinic
Space group	$P\bar{1}$	$P\bar{1}$	$P\bar{1}$	$P\bar{1}$
a / nm	0.962 35(4)	0.959 85(3)	0.956 670(10)	0.985 120(10)
b / nm	1.452 95(5)	1.449 45(4)	1.444 84(2)	1.217 900(10)
c / nm	1.929 82(6)	1.925 38(5)	1.922 04(3)	1.528 57(2)
$\alpha / (^\circ)$	90	90	90	90
$\beta / (^\circ)$	76.529(2)	76.412 0(10)	76.357 0(10)	73.247 0(10)
$\gamma / (^\circ)$	90	90	90	90
V / nm^3	2.458 10(15)	2.436 35(12)	2.411 41(6)	1.653 83(3)
$D_c / (\text{g}\cdot\text{cm}^{-3})$	1.55	1.574	1.62	1.655
Z	2	2	2	2
μ / mm^{-1}	1.144	1.375	2.028	2.909
Data/restraints/parameters	10 971/0/644	10 904/0/644	10 967/0/644	6 334/18/436
$F(000)$	1 168	1 182	1 190	836
GOF	1.043	1.046	1.145	1.063
Final R^{ab} indices ($I>2\sigma(I)$)	$R_1=0.026\ 7$, $wR_2=0.062\ 7$	$R_1=0.027\ 3$, $wR_2=0.061\ 0$	$R_1=0.033\ 8$, $wR_2=0.060$	$R_1=0.032\ 0$, $wR_2=0.075\ 9$
R indices (all data)	$R_1=0.031\ 0$, $wR_2=0.065\ 1$	$R_1=0.032\ 3$, $wR_2=0.062\ 8$	$R_1=0.041\ 7$, $wR_2=0.068\ 9$	$R_1=0.038\ 2$, $wR_2=0.078\ 7$
Reflections collected	13 279	16 968	21 367	9 869
Reflections unique (R_{int})	8 162 (0.015 5)	8 385 (0.029 0)	8 521 (0.023 6)	54 039 (0.018 1)
Refinement method	Full-matrix least-squares on F^2	Full-matrix least-squares on F^2	Full-matrix least-squares on F^2	Full-matrix least-squares on F^2
$(\Delta\rho)_{\text{max}}$, $(\Delta\rho)_{\text{min}} / (\text{e}\cdot\text{nm}^{-3})$	369, -492	572, -800	722, -1178	754, -721

^a $R_1 = \sum ||F_o| - |F_c|| / \sum |F_o|$; ^b $wR_2 = [\sum w(F_o^2 - F_c^2)^2 / \sum w(F_o^2)^2]^{1/2}$.

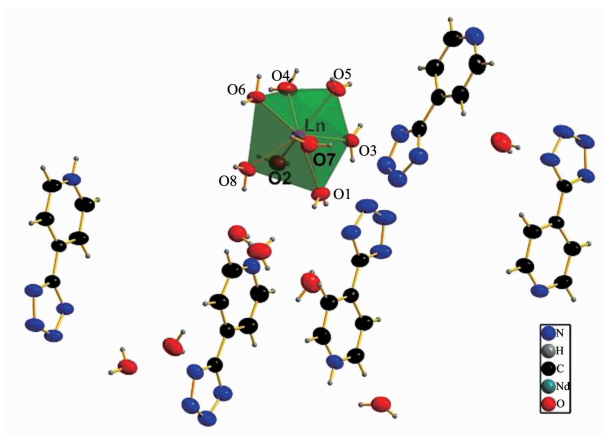
CCDC: 911648,**1**; 942039,**2**; 941826,**3**; 941829,**4**.

2 Result and discussion

2.1 Synthesis and crystal structures of compounds 1~4

The in situ reactions between 4-cyanopyridine (or 3-cyanopyridine), NaN_3 and $\text{Ln}(\text{NO}_3)_3$ offer eight crystalline compounds, $[\text{Ln}(\text{H}_2\text{O})_8 \cdot 3(p\text{-TPD}) \cdot 2(p\text{-HTPD}) \cdot 7\text{H}_2\text{O}]$, ($\text{Ln}=\text{Nd}(\mathbf{1})$, $\text{Eu}(\mathbf{2})$, $\text{Yb}(\mathbf{3})$) and $\text{Ln}(\text{H}_2\text{O})_8 \cdot 3(m\text{-TPD}) \cdot 6\text{H}_2\text{O}$ ($\text{Ln}=\text{Yb}(\mathbf{4})$), respectively. Their IR spectra further confirm the absence of a peak at about $2\,200\text{ cm}^{-1}$, suggesting that the cyano group has turned into the tetrazole group with several typical tetrazolyl group peaks at about $1\,455$, $1\,456$, and $1\,345\text{ cm}^{-1}$ respectively^[2-5].

As shown in table 1, X-ray analysis reveals that compounds **1~3** are isomorphic and crystallizing in the same monoclinic group $P\bar{1}$ and exhibiting the unique frameworks so only the structure of **1** is described in detail here. The asymmetric unit of compound **1** contains one unique La^{III} ion, eight coordinated water molecules, three 4-tetrazoylpyridine ligands ($p\text{-TPD}$), double protonated 4-tetrazoylpyridine ligands ($p\text{-HTPD}$) and seven co-crystallized water molecules. The central metal La^{III} ion is eight-coordinated and has distorted quadrangular prism coordination geometry composed by eight coordinated water molecules. Obviously, two pyridyl groups of different $p\text{-HTPD}$ ligands in the compound are protonated to balance the electric charge (Scheme 1a and Fig.1).

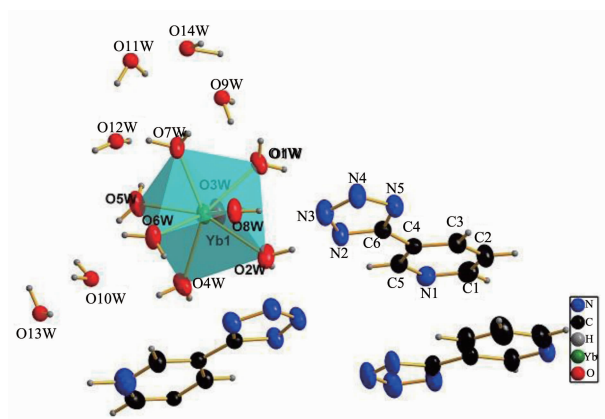


Displacement ellipsoids are drawn at 50% probability level

Fig.1 Polyhedral representation of **1** shows the local coordination geometry around the Ln^{III} center has a slight distorted quadrangular prism

Totally different from compounds **1~3**, compound **4** has other kinds of structure, although both of them also crystallized in the $P\bar{1}$ monoclinic group. As shown in Fig.2, the asymmetric unit of compound **4** contains one unique Ln^{III} ion, eight coordinated water molecules, three 3-tetrazoylpyridine ligands ($p\text{-TPD}$), and six co-crystallized water molecules. Remarkably, on one hand, there are no protonated $m\text{-HTPD}$ ligands in the compounds **4**, on other hand; the number of co-crystallized water molecules is less than that of compounds **1~3** (scheme 1b and Fig.2). The reason why there are so great differences between them is not clear.

There are two kinds of layer constituted the compound **1** (Fig.3). Layer “A” is a cationic layer consisted of part $p\text{-TPD}$ groups and all the central metal cations $[\text{Ln}(\text{H}_2\text{O})_8]^{3+}$ connected by different hydrogen bonds. Layer “B” is an anionic layer constructed by part $p\text{-TPD}$ groups and $p\text{-HTPD}$ groups through hydrogen bonds and $\pi\text{-}\pi$ stacking. As shown in Fig.4a, for layer “A”: the $p\text{-TPD}$ groups and $[\text{Ln}(\text{H}_2\text{O})_8]^{3+}$ building firstly arranged alternately forming a cationic 1-D chain along b -axis by strong inter-molecular hydrogen bonds between the $[\text{Ln}(\text{H}_2\text{O})_8]^{3+}$ building and the tetrazoyl groups $\text{O}(2)\text{--H}(2\text{A})\cdots\text{N}(20)\#3\,0.282\,9(7)\text{ nm}$, and the 1D cationic chain



Displacement ellipsoids are drawn at 50% probability level

Fig.2 Polyhedral representation of **4** shows the local coordination geometry around the Ln^{III} center has a slight distorted quadrangular prism

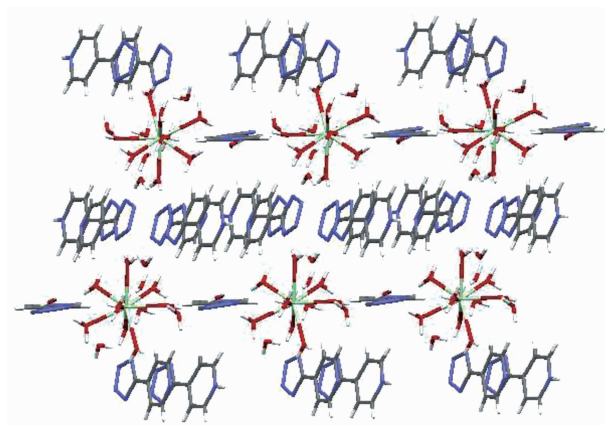
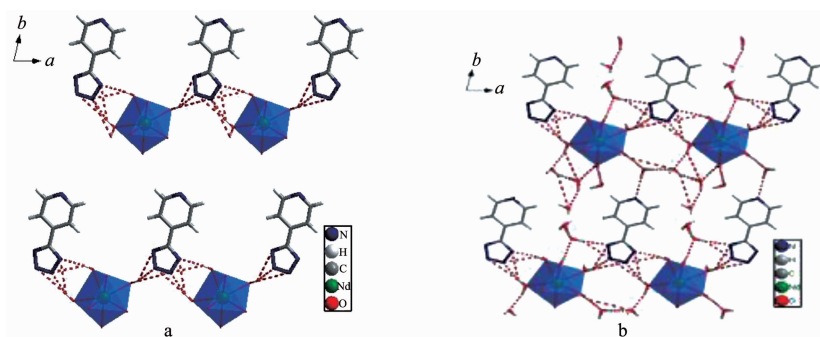


Fig.3 Ionic layers structure of compound **1**



The dotted line indicates hydrogen bonds

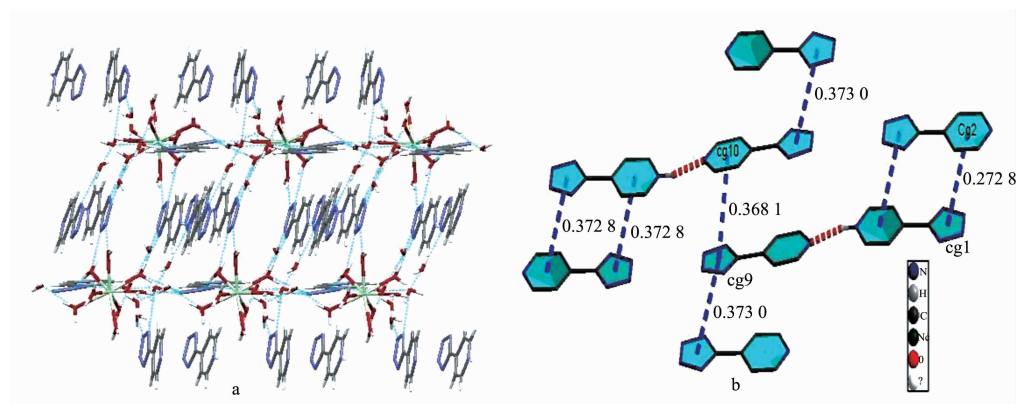
Fig.4 (a) A view of the cationic chains structure connected by hydrogen bonds between coordinated water molecules and tetrazoyl groups along c axis; (b) a view of the cationic layer structure formed by connecting the cationic chains via hydrogen bonds along c axis

then connected to a 2D cationic layer structure via the hydrogen bonds between the co-crystallized water molecules and pyridyl groups ($\text{O}(6\text{W})-\text{H}(6\text{WB}) \cdots$

$\text{N}(16)\#10$ 0.293 9(9) nm), as well as between the coordinated water and co-crystallized water molecules ($\text{O}(5)-\text{H}(5\text{B}) \cdots \text{O}(1\text{W})\#5$ 0.262 9(6) nm) (Fig.4b). For

layer B; another intermolecular hydrogen bonds between protonated pyridyl groups and pyridyl groups (N(6)-H(6)⋯N(21)#1 0.266 5(7) nm; N(1)-H(1)⋯N(11) #2 0.270 5(7) nm) and the vertical offset face to face π - π stocking effect link the *p*-HTPD and *p*-TPD anions in the formation of the anionic layer structure (Fig.5). Take the π - π stocking effect between plane cg9 and cg10 for example (cg indicate plane number), atoms N22, N23, N24, N25 and C30 constituted plane

cg9, N21, C25, C26, C27, C28 and C29 constituted plane cg10. The distance between the two centroids is 0.368 nm, dihedral angle 4.01° (Fig.5 (b)). The π - π stacking interactions and hydrogen bonds among the coordinated water, co-crystallized water, *p*-TPD and *p*-HTPD groups and offset face to face stocking effect are speculated to assembly the molecules into a three dimensional structure (Table S I and Fig.6).



Dashed lines indicate hydrogen bonds and π - π stacking effect

Fig.5 (a) 3D supermolecular structure of compound **1** connected by hydrogen bonds and π - π stacking; (b) an example of the π - π stacking between pyridyl and 4-tetrazoyl groups and intermolecular protonated pyridyl groups to pyridyl groups hydrogen bonds of the anionic layer

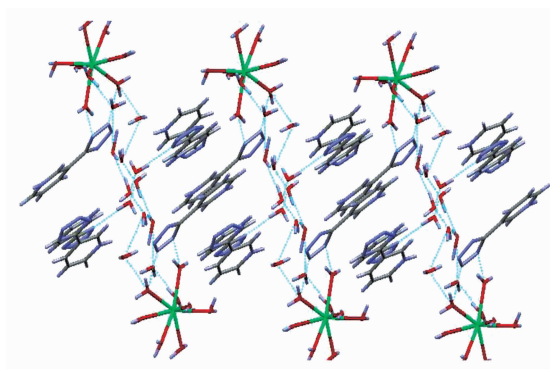
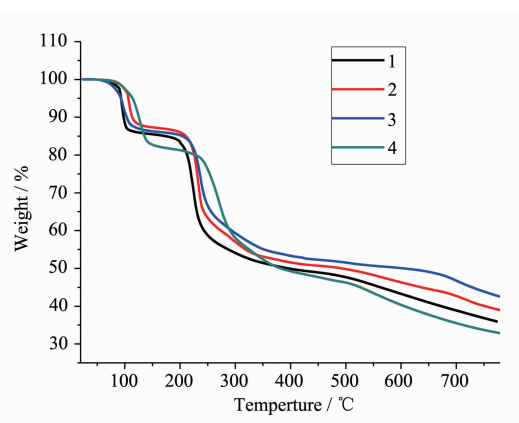


Fig.6 Supermolecular structure of compound **4** viewed from *c* axis

2.2 Thermo-gravimetric analysis of 1~4

As shown in Fig.7, upon careful examination on the thermo-gravimetric curves of compounds **1**~**4**, we found all the thermo-gravimetric curves of compounds have almost the similar graphic: such as for **1**, the first clean weight loss “step” just happened from 70 to 120 °C (*ca.* 11.90%) and the second weight loss occurred from 180 to 230 °C. This can be attributed to

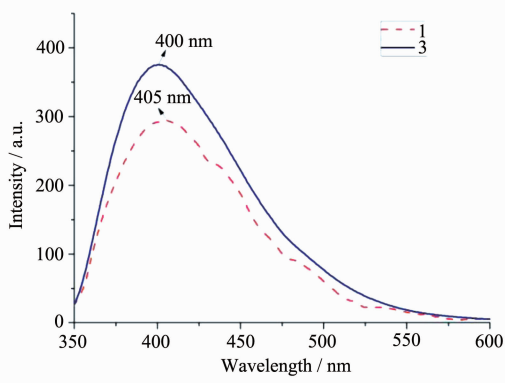
the removal of co-crystallized water molecules from the compounds **1** (Calcd. for compound **1**, 11.03%), and the second one in 180 ~230 °C is due to the decomposed of the whole structure according to the TGA data. Similar to that of compounds **1**~**3**, there are two clean weight loss “step” in the thermo gravimetric curves of **4**, the first weight loss “step” just happened from 70 to 120 °C (*ca.* 14.5%) and the second weight

Fig.7 Thermo gravimetric analysis(TGA) of **1~4**

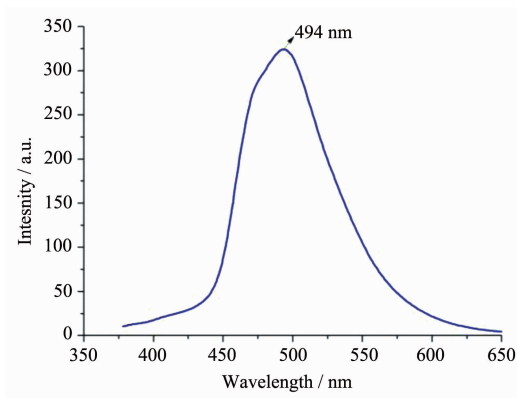
loss occurred from 180 to 230 °C, The first weight loss “step” are also attributed to the removal of co-crystallized water molecules from the compounds **4** (Calcd. 12.6%). Beyond the 230 °C, the compounds decomposed.

2.3 Fluorescence property

As shown in Fig.8, the solid-state fluorescence spectra (a Perkin-Elmer LS50B) that were used for measurement of crystalline samples for **1** and **3** at room temperature indicate the maximal emission peaks occur in 405 and 400 nm respectively (with $\lambda_{\text{ex}}=309$ nm), suggesting compound **1** and **3** may be good blue light emitting material. The photo-luminescent mechanism is tentatively attributed to ligand-to-ligand ($\pi \rightarrow \pi^*$) transitions that are in reasonable agreement with literature examples on this class of metal complex previously reported in our group and by others^[5,9]. A little difference of the wavelength between **1** and **3** are caused by the different central Ln metals with different

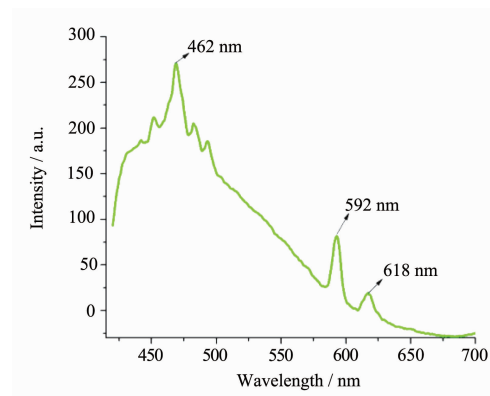
Fig.8 Solid state photo-luminescent spectrum of compound **1** and **3** at room temperature

supermolecular interaction. The same to compounds **1** and **3**, the solid-state fluorescence spectra for **4** (Fig.9) at room temperature show the maximal emission peaks occur in 494 nm respectively (with $\lambda_{\text{ex}}=375$ nm), suggesting compound **4** may be good green light emitting material. The large differences of maximal emission peaks between **4** and **1** can be attributes to

Fig.9 Solid state photo-luminescent spectrum of compound **4** at room temperature

their different reaction substrate.

Totally different from compound **1**, **3** and **4**, as shown in Fig.10, when excited at 394 nm, compound **2** emit a series of emission peaks at 618, 592 and 462 nm respectively in near-infrared luminescent field at room temperature (Fig.10). Compared by the complexes $[\text{KEu}(\text{suc})_{0.5}(\text{ox})_{1.5}(\text{H}_2\text{O})] \cdot \text{H}_2\text{O}$ et al^[20-22], we can conclude the emission peaks of 592 and 618 nm is tentatively assigned to the $D \rightarrow F$ transition 592 nm ($^5D_4 \rightarrow ^7F_1$), 618 nm ($^5D_4 \rightarrow ^7F_2$) in europium atoms^[20]. In addition, another intense emission is 462 nm for **2**, which implies green emission light can be attributed

Fig.10 Solid state photo-luminescent spectrum of compound **2** at room temperature

to the $\pi \rightarrow \pi^*$ or $n \rightarrow \pi^*$ transition of tetrazoly and pyridyl groups of the ligands.

Supporting information is available at <http://www.wjhxxb.cn>

References:

- [1] Demko Z P, Sharpless K B. *J. Org. Chem.*, **2001**,**66**:7945-7950
- [2] Fu D W, Zhang W, Xiong R G. *Cryst. Growth Des.*, **2008**,**8**:3461-3464
- [3] Tang Y Z, Huang X F, Song Y M, et al. *Inorg. Chem.*, **2006**,**45**:4868-4870
- [4] Ye Q, Song Y M, Fu D W, et al. *Cryst. Growth Des.*, **2007**,**7**(9):1568-1570
- [5] Tang Y Z, Tan Y H, Liu D L, et al. *Inorg. Chim. Acta*, **2009**,**362**(6):1969-1973
- [6] Zhao H, Qu Z R, Ye H Y, et al. *Chem. Soc. Rev.*, **2008**,**37**:84-100
- [7] Hang T, Zhang W, Ye H Y, et al. *Chem. Soc. Rev.*, **2011**,**40**:3577-3598
- [8] Ye Q, Song Y M, Wang G X, et al. *J. Am. Chem. Soc.*, **2006**,**128**(20):6554-6555
- [9] Li Z, Li M, Zhou X P, et al. *Cryst. Growth Des.*, **2007**,**7**(10):1992-1998
- [10] Sengupta O, Mukherjee P S. *Inorg. Chem.*, **2010**,**49**(18):8583-8590
- [11] Tang Y Z, Cao Z, Wen H R, et al. *J. Coord. Chem.*, **2010**,**63**(17):3101-3107
- [12] Gálvez-Ruiz J C, Holl G, Karaghiosoff K, et al. *Inorg. Chem.*, **2005**,**44**(12):4237-4253
- [13] Ouellette W, Prosvirin A V, Whitenack K, et al. *Angew. Chem. Int. Ed.*, **2009**,**48**:2140-2143
- [14] Lee H H, Han S Y, Gyoung Y S, et al. *Inorg. Chim. Acta*, **2011**,**378**:174-185
- [15] Liang L, Peng G, Ma L, et al. *Cryst. Growth Des.*, **2012**,**12**(3):1151-1158
- [16] Sheldrick G M. *SADABS. Version 2.05*, University of Göttingen Germany, **2002**.
- [17] *SHELXTL 6.10*, Bruker Analytical Instrumentation, Madison, Wisconsin, USA, **2000**.
- [18] Jha P, Bobev S, Subbanna G N, et al. *Chem. Mater.*, **2003**,**15**(11):2229-2233
- [19] Liu J P, Wilding W V, Giles N F, et al. *J. Chem. Eng. Data*, **2010**,**55**(1):41-45
- [20] Zhang X J, Xing Y H, Han J, et al. *Cryst. Growth Des.*, **2008**,**8**(10):3680-3688
- [21] Manseki K, Hasegawa Y, Wad Y, et al. *J. Lumin.*, **2005**,**111**(3):183-189
- [22] Zhang W, Liu L, Wen S P, et al. *J. Rare Earths*, **2006**,**24**(1):9-13